CellPress
Partner Journal

Molecular Plant
Research article

Convergent antisense transcription primes hosting genes for stress responsiveness in plants

Vasiliki Zacharaki[1,7], Marti Quevedo[2,3,7], Sarah Muniz Nardeli[2,5,7], Shiv Kumar Meena[1,6], Elena Monte[3,4] and Peter Kindgren[1,*]

[1]Umea Plant Science Centre, Department of Forest Genetics and Plant Physiology, Swedish University of Agricultural Sciences, 90187 Umea, Sweden

[2]Umea Plant Science Centre, Department Plant Physiology, Umeå University, 90187 Umea, Sweden

[3]Centre for Research in Agricultural Genomics, CRAG (CSIC-IRTA-UAB-UB), Campus UAB, Cerdanyola del Vallès, Spain

[4]Consejo Superior de Investigaciones Científicas (CSIC), Barcelona, Spain

[5]Linnean Center for Plant Biology, Department of Plant Biology, Swedish University of Agricultural Sciences, 75007 Uppsala, Sweden

[6]Present address: National Institute of Plant Genome research, Aruna Asaf Ali Marg, New Delhi 110067, India

[7]These authors contributed equally to this article.

***Correspondence: Peter Kindgren (peter.kindgren@slu.se)**

https://doi.org/10.1016/j.molp.2025.10.001

ABSTRACT

Plants need to constantly surveil their surroundings to adapt to environmental fluctuations, which they achieve primarily through transcriptional reprogramming. Thus, plants are excellent models for identifying novel transcriptional regulatory mechanisms. In this study, we characterize the regulation mediated by long non-coding transcription that initiates on the complementary strand in the 5' end of coding genes (convergent antisense transcription, CASt). In *Arabidopsis*, CASt is associated with stress-responsive genes that are highly expressed. Our analysis shows that CASt depends on a specific gene architecture that is evolutionarily conserved in higher plants. CASt is present in genes with an extended first intron and over-represented in genes encoding functional transporters in *Arabidopsis*, such as the AMINO ACID PERMEASE (AAP) transporter family. Experimental evidence points to a role for CASt in priming their host genes for stress responsiveness in evolutionary divergent plant species. Furthermore, we were able to predict stress responsiveness in rice AAP genes based on the presence of a long first intron and CASt. Collectively, we show an evolutionary strategy and regulatory mechanism specific to plants for enhancing stress responsiveness through modification of gene architecture and antisense transcription.

Key words: *Arabidopsis*, antisense transcription, cold acclimation, transporters

Zacharaki V., Quevedo M., Nardeli S.M., Meena S.K., Monte E., and Kindgren P. (2025). Convergent antisense transcription primes hosting genes for stress responsiveness in plants. Mol. Plant. **18**, 1920–1931.

INTRODUCTION

Plant stress responses involve several layers of regulation, including complex transcriptional mechanisms. Detecting fast changes in transcription is crucial for understanding how plants rapidly adapt to environmental challenges. However, many transcriptional events are difficult to detect by steady-state methods due to the rapid degradation of the synthesized RNA. Efficient approaches for directly studying all genome-wide transcription events measure active transcription by RNA polymerase II (RNAPII), the primary RNA polymerase in eukaryotic cells. For example, native elongation transcript sequencing (NET-seq) captures the RNA attached to RNAPII and can detect transcription events before degradation occurs. This enables the detection of transcripts that are normally rapidly turned over (i.e., non-coding transcripts) (Churchman and Weissman, 2011; Kindgren et al., 2019). NET-seq in plants (plaNET-seq) has previously identified one class of long non-coding transcription, defined as convergent antisense transcription (CASt) (Kindgren et al., 2019). *Arabidopsis thaliana* possesses two types of antisense transcription to a large degree, defined as CASt and poly(A)-associated antisense transcription (PASt; initiates in the 3' end of genes) (Kindgren et al., 2019). We have previously characterized PASt in *Arabidopsis*, and it occurs frequently at stress-responsive transcription factors (Meena et al., 2024). However, despite being prominent in eukaryotic genomes, antisense transcription is poorly studied.

CASt in *Arabidopsis*, as in metazoans, is often initiated at the first exon–intron junction (Brown et al., 2018). Additionally, CASt in *Arabidopsis* is detected at genes that display a certain 5'-end gene structure and have, on average, a long first exon and intron

(Kindgren et al., 2019). First introns harbor important DNA sequences that dictate the expression of their host genes (Zalabák and Ikeda, 2020). In human cells, the DNA sequences of the first intron are the longest and most conserved compared to other introns (Le Hir et al., 2003; Park et al., 2014; Jo and Choi, 2019). In plants, first introns are important determinants of proper stress response, mostly being described in the process of alternative splicing (Mastrangelo et al., 2012; Jabre et al., 2019). However, how stress-responsive CASt influences the expression of their long first intron-containing host genes is unknown.

In the present study, we found that *Arabidopsis thaliana* genes harboring CASt predominantly encode stress-responsive transporters. Transporters orchestrate plant stress responses by a rapid modulation of the influx and efflux of cellular components. For instance, the distribution of nitrogen is partly controlled by the amino acid/auxin permease (AAAP) family, a widely diverse superclass of transporters including AMINO ACID PERMEASE (AAP) and LYSINE-HISTIDINE-LIKE TRANSPORTERS (LHT) families (Tegeder and Ward, 2012). However, not all AAAPs in a subclass have CASt, suggesting specialization and a unique evolutionary pressure for some members. We reveal a confluence of CASt into an extended first intron within specific members of a protein family. Experimental evidence shows that the combination of regulatory elements in the first intron and proper CASt of *AMINO ACID PERMEASE 1* (*AAP1*) play a role in the gene's ability to respond to cold stress. Moreover, we showed that the presence of CASt at *AAP* transporters and low-temperature responsiveness is conserved in maize and rice, evolutionary distant plant species. Our study reveals CASt as an evolutionary conserved regulatory mechanism to prime plant genes for stress response.

RESULTS

CASt genes predominantly encode stress-responsive transporters

CASt has earlier been detected and defined in *Arabidopsis* (Kindgren et al., 2019). They are non-coding transcription events that initiates at the 5' half of their host gene (CASt genes, Supplemental Table 1), with over 90% of CASt initiating around the first or second exon–intron junction (Figure 1A) (Kindgren et al., 2019). CASt is often rapidly degraded in the plant cell, and a nascent sequencing method is required to detect the transcription events (Kindgren et al., 2019); an example can be seen in Figure 1B. To further characterize CASt genes, we measured their length. CASt genes were longer compared to expressed genes (Figure 1C) and included a significantly longer first intron (median of 342 bp) compared to non-CASt genes (median of 202 bp) (Supplemental Figure 1A). These features made us evaluate whether there was evolutionary pressure on the DNA region that includes the first intron and where CASt is active. Thus, we calculated PhyloP scores, which measure evolutionary conservation at individual alignment sites (high values mean sequences are predicted to be more conserved). We detected an increased positive PhyloP score for CASt genes (Figure 1D, dashed box), suggesting that the interval where CASt is initiated is an evolutionary feature in plants.

To better understand the biological importance of hosting CASt, we performed a Gene Ontology (GO) analysis. CASt genes were enriched in those encoding transporters (Figure 1E, Supplemental Table 2) and for terms related to the response to different kinds of stimuli, including abiotic stress (Figure 1F, Supplemental Table 2). 111 genes have previously been assigned a transport role in the list of CASt genes (Supplemental Table 3). For example, *AVTJ1* has previously been described as a salt-responsive transporter gene (Gong et al., 2001). *AVTJ1* is defined as a CASt gene with a long first intron, and we confirmed that *AVTJ1* is responding to low temperature with plaNET-seq data (Supplemental Figure 1B). We evaluated whether a long first intron alone could explain the stress responsiveness in CASt genes. On the contrary, genes with a long first intron but without CASt had different, non-stress-related terms over-represented compared to CASt genes (Supplemental Table 4). Corroborating these results, the first introns of CASt genes compared to the first introns of non-CASt genes with a long first intron were not enriched for stress-related regulatory DNA elements (Supplemental Figure 1C, Supplemental Table 5). However, when we compared the full-length sequence of CASt genes including the promoter to expressed genes, we found a plethora of known stress-involved regulatory motifs enriched (Supplemental Figure 1D). Together, this indicates that the first introns of CASt genes are evolutionary conserved but not preferentially occupied by *cis*-regulatory elements involved in stress response. It further suggests that the long first introns with CASt have evolved side by side with regulatory motifs in the rest of the gene body and promoter to make the gene stress responsive.

CASt genes are highly active in normal growth conditions and responsive to cold stress

CASt has previously been found to be highly cold responsive with transcriptional activity decreasing after 3 and 12 h at 4°C compared to 22°C (Kindgren et al., 2019). To further characterize the effects of CASt in the transcription regulation of their host genes, we evaluated their chromatin context using available genome-wide datasets. First, we detected a higher polymerase (RNAPII) occupancy at CASt loci compared to the control set (Figure 2A). Second, chromatin accessibility assessed by the assay for transposase-accessible chromatin with sequencing (ATAC-seq) corroborated that CASt genes have an open chromatin environment over the promoter and 5' end, suggesting that CASt genes were highly active in normal growing temperatures (Figure 2B). High-resolution genome-wide nascent transcription data are so far only available after low-temperature (4°C) treatment (Kindgren et al., 2019). Therefore, we focused our analysis on this stress condition. Indeed, when looking at sense transcription, we validated that CASt genes have enhanced low-temperature response when compared with genes without CAS transcription that were actively induced after 3 h at 4°C (Supplemental Table 6). Additionally, we plotted plaNET-seq data centered on the +1 nucleosome and CASt genes showed an augmented RNAPII stalling (Figure 2C and 2D), indicating that CASt genes are in a "stand-by" state for activation at 22°C. We observed that genes without antisense transcription had a symmetric stalling around the first nucleosome. In contrast, at CASt genes, we observed an increased RNAPII occupancy downstream of the stalling site compared to upstream, indicating increased transcriptional activity along the gene body. A similar pattern was detected when plotting active RNAPII transcription after 3 h

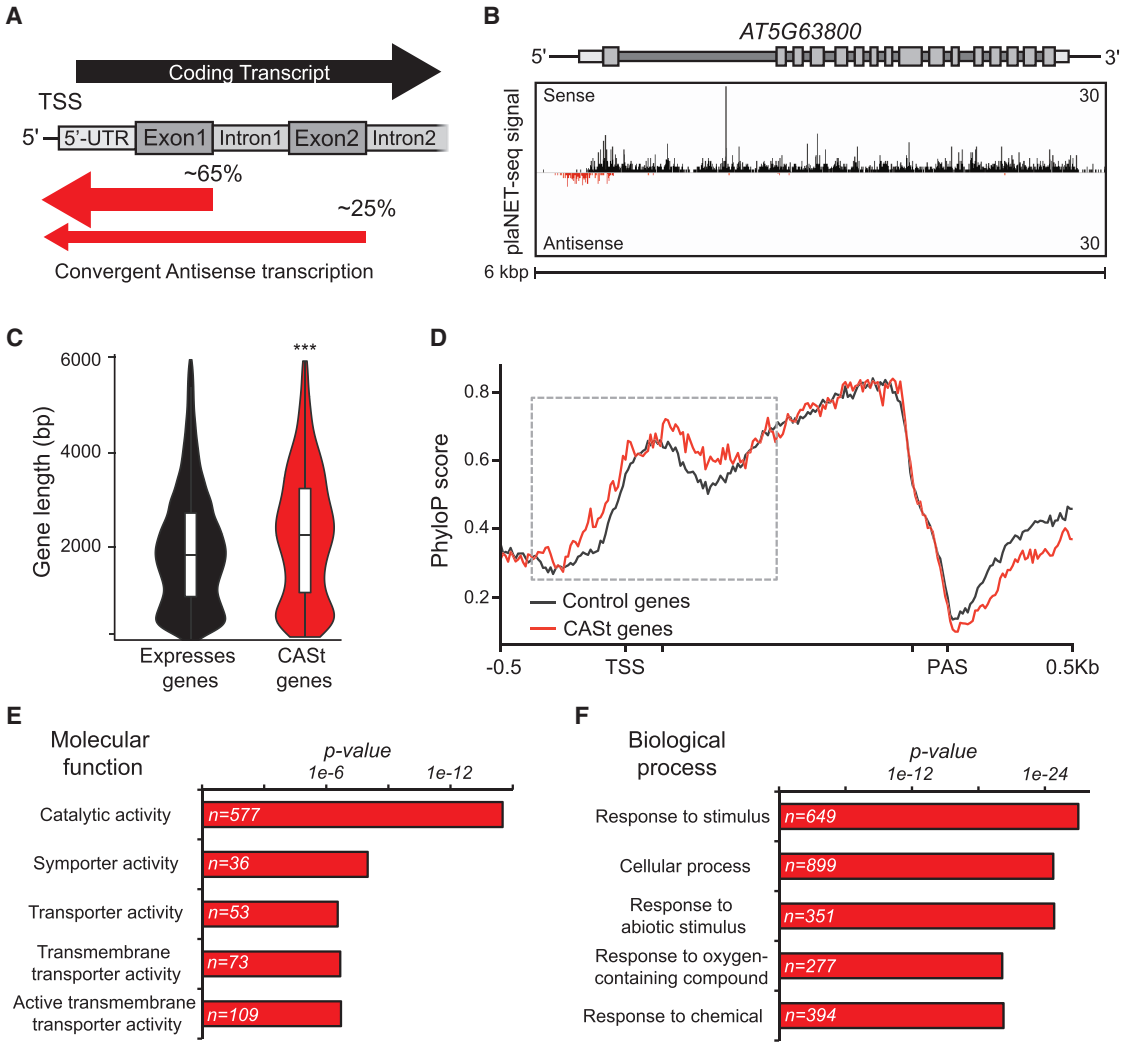

Figure 1. CASt genes predominantly encode stress-responsive transporters.

(A) Graphical illustration of the definition of convergent antisense transcripts (CAS).

(B) plaNET-seq screenshot of a CASt gene, *AT5G63800*.

(C) Violin plot of the length of all expressed genes compared to CASt genes. *p* value (1.19e−11) was calculated with the Mann-Whitney U test.

(D) Average conservation using PhyloP scores calculated from 63 plant species across control genes or CASt genes. The coverage of scores is unscaled from 500 bp upstream of the transcription start site (TSS) coordinate and downstream of the polyadenylation signal (PAS). Regions between TSS and PAS are scaled.

(E and F) GO term enrichment (top 5) of CASt genes **(E)** molecular function and **(F)** biological processes. The numbers indicate the detected number of genes in respective GO term.

at 4°C (Figure 2E and 2F). The low-temperature response was greatly enhanced in CASt genes compared to upregulated genes without antisense transcription. Thus, our data strongly suggest that CASt genes have an enhanced response to 4°C compared to upregulated genes without antisense transcription. This "ready state" of low-temperature regulation at control temperatures indicates that a main function for CASt is already active at 22°C.

CASt as a mechanism of evolutionary divergence in amino acid transporters

To further investigate the biological role of CASt in their host genes, we explored the list of CASt genes with transporter function and divided them into their protein families (Supplemental Figure 2A) (Fischer et al., 1998; Li et al., 2002; Ahn et al., 2004; Maurino et al., 2006; Kang et al., 2011; Jelesko, 2012; Denancé et al., 2014; Niño-González et al., 2019; Hao et al., 2020; Ji et al., 2022). We noted that relatively few genes from each investigated family hosted CASt. The highest occurrence was found in the AAAP family (11 CASt genes of 44 total members), warranting further analysis. We observed that the few genes hosting CASt in each AAAP subclass coincidently presented the longest first intron among its members (Figure 3A, Supplemental Figure 2B–2E). This phenomenon was also found in other transporter families (Supplemental Figure 2F and 2G), indicating a general gene-architecture specialization for some members in distinct subclasses in *Arabidopsis*. To evaluate

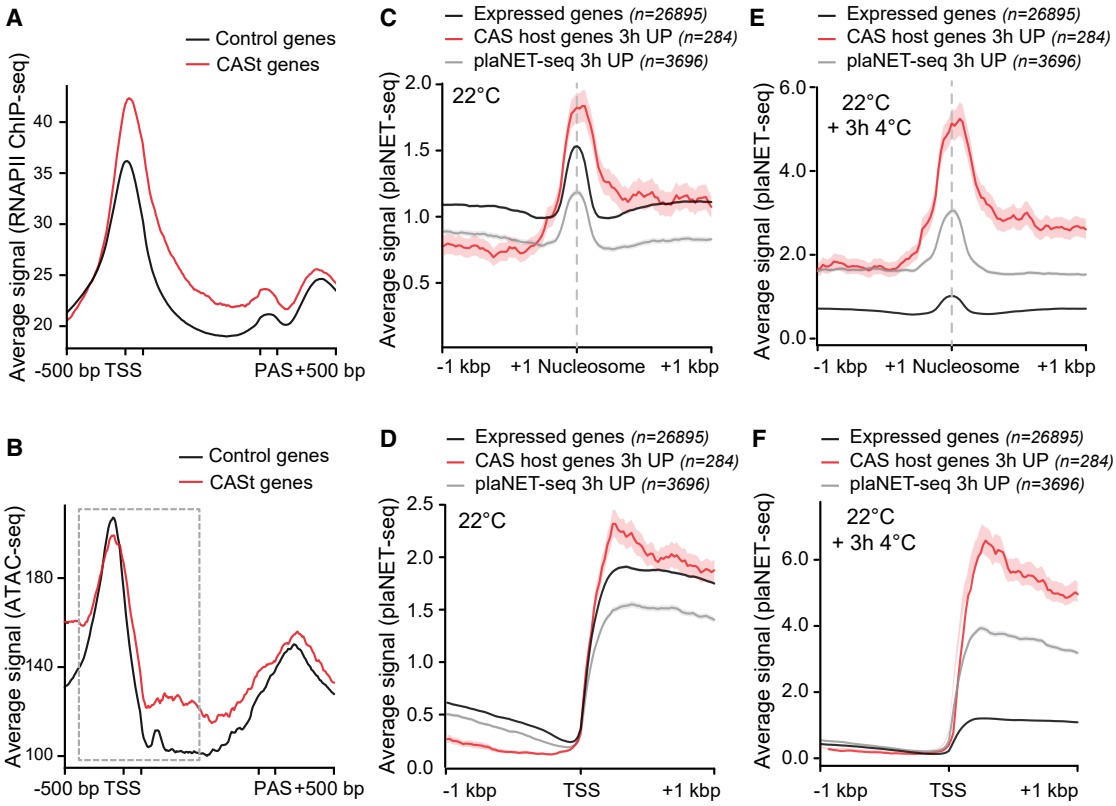

Figure 2. CASt genes are active and highly responsive to stress.

(A) Metagene profile of RNAPII chromatin immunoprecipitation sequencing data.

(B) Metagene profile of ATAC-seq data along the whole scaled gene body, with unscaled plotting from 500 bp upstream of the transcription start site (TSS) coordinate and downstream of the polyadenylation signal (PAS).

(C and D) Metagene profile of plaNET-seq data at 22°C centered on the **(C)** +1 nucleosome and **(D)** TSS of CASt genes (UP 3h at 4°C), compared to non-responding genes, and other upregulated genes at 3h 4°C without antisense transcription.

(E and F) Metagene profile of plaNET-seq data at 3 h at 4°C centered on the **(E)** +1 nucleosome and **(F)** TSS of CASt genes (UP 3 h at 4°C), compared to non-responding genes, and other upregulated genes at 3 h at 4°C without antisense transcription.

whether AAAP CASt genes in *Arabidopsis* were generally responding to stress, we used published plaNET-seq data at control (22°C) temperature and during low-temperature exposure. All but one CASt gene showed significant changes in cold stress, while none of the genes without CAS transcription responded to low temperature (examples can be seen in Supplemental Figure 3). Together, these results pinpoint long introns, and their hosted CASt, as a possible mechanism of divergent regulation between members of a gene family.

The AAP family mediates uptake and distribution of amino acids across plant tissues, thereby playing central roles in nitrogen allocation, seed development, and plant growth, yet their role in cold stress response has not been explored. Within this family, two genes hosted CASt. AAP1 is primarily involved in amino acid import during early seedling development and contributes to nitrogen partitioning, while AAP5 functions in the uptake of cationic amino acids and regulates amino acid homeostasis, especially under stress and during root-to-shoot transport (Lee et al., 2007; Svennerstam et al., 2008, 2011). Both genes belong to subclasses with multiple members. Thus, we chose these CASt genes for a more detailed analysis (Figure 3A). The amino acid sequence of the six AAPs is highly conserved between members, supporting their common ancestry, but their gene structure is highly variable (Supplemental Figure 2H–2I). Our analysis showed that *AAP1* and *AAP5*, and their CASt, are highly responsive to low temperature at a steady state and nascent level (Figure 3B–3E). In contrast to their host gene, the CASt of *AAP1* (*asAAP1*) and *AAP5* (*asAAP5*) was downregulated during cold stress (Figure 3D and 3E, Supplemental Figure 4A and 4B). Available cap analysis of gene expression (CAGE) and direct RNA sequencing (DRS-seq) data showed the start and end of CASt at *AAP1* and *AAP5* (Supplemental Figure 5A and 5B). CASt initiates at the fourth and second exon–intron junctions, respectively. Both transcripts had an increased CAGE signal in *hen2-2* and *rrp4-2* mutants, indicating a rapid turnover by the nuclear exosome. Thus, our analysis pinpoints AAP1 and AAP5 as novel players in the low-temperature response and CASt as a putative mechanism of their regulation.

AAP1 and AAP5 are involved in amino acid homeostasis in response to low temperature

Although AAP1 and AAP5 have not previously been linked to the low-temperature response, the polyamines they transport are well known to contribute to abiotic stress tolerance, including cold stress (Chen et al., 2019; Ramazan et al., 2023; Blázquez, 2024). To test their biological function, we used transfer DNA

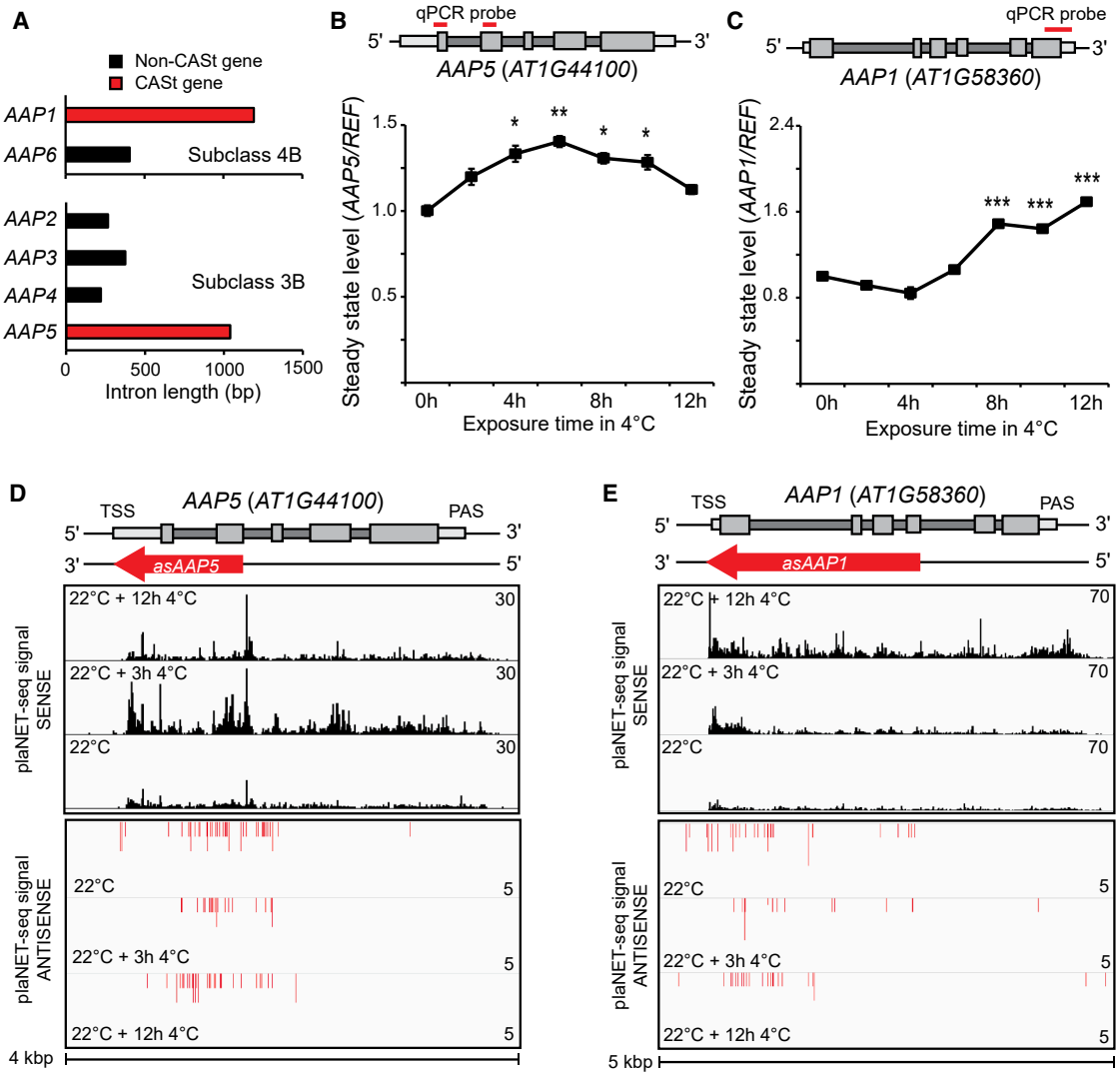

Figure 3. Members in the AAAP transporter gene family present a long first intron.

(A) The length in base pairs of the first intron in members of the *AAP* class.

(B and C) The relative steady-state level measured by RT–qPCR following exposure to 4°C at indicated time points of 10-day-old seedlings of **(B)** *AAP5* and **(C)** *AAP1*. Steady-state levels were normalized to WT levels at 22°C. The mean values are from three biological replicates. Error bars represent ±SEM. Statistical significance was calculated with Student's *t-test* (*$p < 0.05$, **$p < 0.01$, ***$p < 0.001$).

(D and E) Graphical illustration of the gene (upper panel), plaNET-seq screenshots of sense transcription (black, middle panel), and plaNET-seq screenshots of antisense transcription (red, lower panel) of **(D)** *AAP5* and *AT1G44100* and **(E)** *AAP1* and *AT1G58360*.

(knockout) mutant lines of *AAP1* and *AAP5*. To assess growth at low temperature, we compared plants that stayed in 22°C with plants moved to 10°C (growth at 4°C is minimal, hence the use of 10°C). Both *aap* mutants showed impaired growth at 10°C (Figure 4A and 4B) and increased tolerance to freezing after cold acclimation compared to wild type (WT) (Supplemental Figure 6A). This tradeoff effect between growth and freezing tolerance is a common phenotype in mutants impaired in the low-temperature response in *Arabidopsis* (Jaglo-Ottosen et al., 1998; Gilmour et al., 2000).

In addition, we performed a relative growth rate (RGR) assay (Nunes et al., 2013) and found that loss of AAP5 resulted in increased plant growth boost after plants returned to 22°C compared to WT (Supplemental Figure 6B). *app1-3* mutants recovered with a delay compared to WT plants with a peak at 11 h. Plants that grew continuously at 22°C had no significant differences (Supplemental Figure 6C). To confirm that there was an imbalance in polyamine content after short-term low-temperature exposure in our mutants, we measured the metabolic composition of polyamines, their precursors, and their derivatives. Glutamate in the form of glutamic acid had an overall lower concentration in both mutants compared to the WT (Figure 4C). Both AAP1 and AAP5 transport glutamate and it is a key metabolite for all polyamines (Boorer and Fischer, 1997; Perchlik et al., 2014). Glutamic acid has been implicated as an important molecule in the low-temperature response in plants (Barand et al., 2015; Lee et al., 2021). Additionally, we observed a misregulation of the levels of other polyamines in response to low temperature in the mutants (Figure 4D,

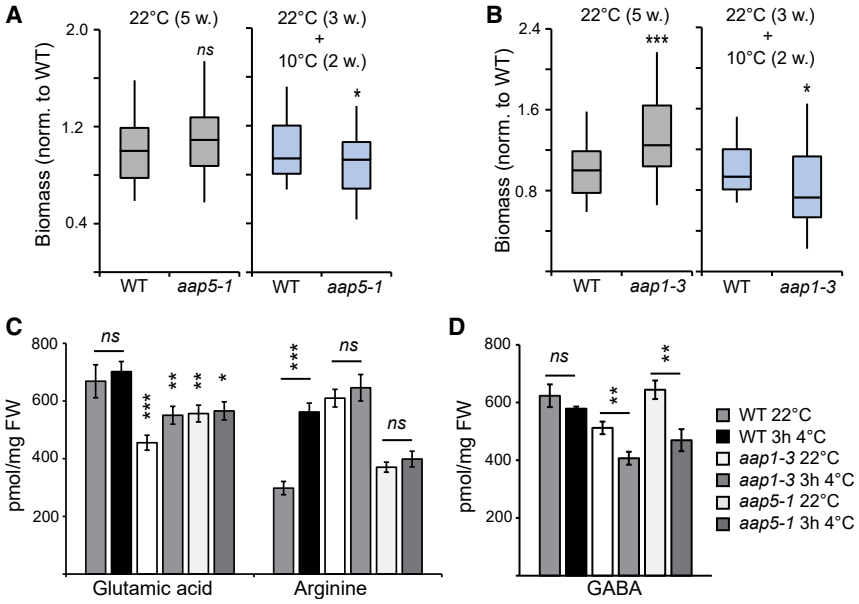

Figure 4. *AAP5* and *AAP1* are cold responsive and important for plant growth at low temperatures.

(A and B) The relative weight (wet) of WT and mutant plants after 5 weeks at 22°C and after 3 weeks at 22°C and 2 weeks at 10°C for **(A)** *aap5-1*, and **(B)** *aap1-3*. Statistical significance was calculated with Student's *t-test* (*$p < 0.05$, ***$p < 0.001$).

(C and D) Concentration of glutamic acid and arginine **(C)** and GABA **(D)** in WT, *aap5-1*, and *aap1-3* seedlings grown for 10 days. Samples were taken at 22°C and after 3 h at 4°C. Each bar represents at least five biological replicates. Error bars represent ±SD. Statistical significance was calculated with Student's *t-test* (*$p < 0.05$, **$p < 0.01$, ***$p < 0.001$).

Supplemental Figure 7). Taken together, our data show that AAP1 and AAP5 are important for the low-temperature response in *Arabidopsis*.

Impaired CASt correlates with a loss of AAP1 induction after exposure to low temperature

Next, we tested the impact of CASt in the low-temperature response on their hosting genes. We aimed to generate stable CRISPR-Cas9 deletion lines where parts of the first intron of *AAP1* and *AAP5* would be deleted. We were unable to attain *AAP5* lines but succeeded for *AAP1* (*aap1-cr*, Figure 5A). Our isolated line fulfilled two important criteria. Firstly, we did not interfere with the transcription start site (TSS) of the CAS (*asAAP1*). Secondly, we did not interfere with the expression of sense *AAP1* at control conditions (Figure 5B), nor did we interfere with the splicing or stability of sense *AAP1* mRNA (Supplemental Figure 6). When seedlings were exposed to low temperature, we did not detect an induction of *AAP1* steady-state levels in *aap1-cr* (Figure 5B). In addition, we detected lower levels of *asAAP1* in *aap1-cr* in control conditions compared to WT and did not detect any low-temperature-induced response (Figure 5C). This suggests that the deleted sequence of the first intron is important for regulation of *asAAP1* rather than *AAP1* at 22°C. During exposure to 4°C, the deleted sequence is important for stress-induction of *AAP1* and repressing *asAAP1* expression. The *aap1-cr* mutant showed a similar cold-sensitive growth phenotype to the *aap1* mutant, indicating that impaired low-temperature response in *aap1-cr* has a biological role (Figure 5D). The results from *aap1-cr* corroborate our hypothesis that *asAAP1* and regulatory sequences in the first intron are required for proper regulation of *AAP1*. It also suggests that the expression of *asAAP1* partly dictates the regulation of the host gene.

CASt are found concurrently across plant evolution

An interesting question derives from our results in *Arabidopsis*: has the mechanism of low-temperature response via CASt and long first intron emerged in specific transporters in other plant species? We first retrieved the sequence of the AAP family in different species of the green lineage; a chlorophyte (*Coccomyxa subellipsoidea*), two bryophytes (*Physcomitrella patens* and *Marchantia polymorpha*), and a lycophyte (*Selaginella moellendorffii*) (Zhang et al., 2020). We also included four higher plants; *Arabidopsis thaliana* (Tegeder and Ward, 2012), *Oryza sativa* (Taylor et al., 2015), *Populus trichocarpa* (Bai et al., 2019), and *Zea mays* (Islam et al., 2024). Comparative analysis showed that at least one member of the AAP family had an extended intron compared with the other members, suggesting a targeted selection of a long first intron in all species investigated (Figure 6A, Supplemental Table 7). The occurrence of long first introns was more prevalent in higher plants, indicating that this evolutionary strategy is more common among these species. To confirm this, we used available precision run on sequencing data in maize and rice to identify CASt (Joly-Lopez et al., 2020; Lozano et al., 2021). We chose subclasses with multiple expressed members (only one subgroup in maize and three in rice) with and without CASt. This made it possible to investigate genes where their encoded amino acid sequences are highly similar but with different gene structures. Similar to *Arabidopsis*, maize and rice genes with the longest first intron in each subclass had an associated CASt (Supplemental Figures 9 and 10). For example, the CASt gene *ZmAAP6* has been shown to respond strongly to drought compared to the other subgroup members (Islam et al., 2024). In rice, the expression of all genes in Supplemental Figure 9 was monitored with RT–qPCR in control and after 4°C exposure (*OsAAP14*, *OsAAP5*, *OsAAP17*, and *OsAAP2* were not detectable in our conditions). In perfect alignment with our hypothesis, all CASt genes in rice were more responsive to cold stress than their close homologs without antisense transcription (Figure 6B). This indicates that the AAP family of transporters has been under evolutionary pressure to adopt a member-specific gene structure, tightly correlated to their low-temperature responsiveness. Collectively, our study highlights the conservation of gene architecture across evolutionary divergent plant species and points to a general role for CASt to prime transporter genes for the response to low temperature.

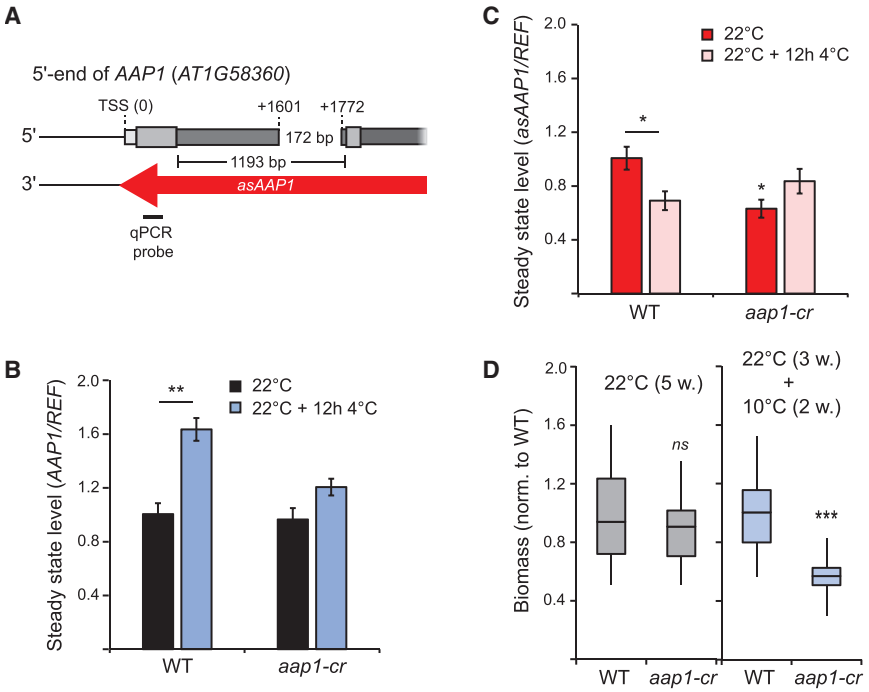

Figure 5. Characterization of the *aap1-cr* mutant.

(A) Graphical illustration of the position of the deletion in *aap1-cr*. The qPCR probe used for amplification of *asAAP1* in **(D)** is shown.

(B) The relative steady-state level measured by RT–qPCR at 22°C and following low-temperature exposure (12 h at 4°C) of *AAP1* in WT and *aap1-cr* seedlings grown for 10 days. Steady-state levels were normalized to WT levels at 22°C. The mean values are from three biological replicates. Error bars represent ±SEM. Statistical significance was calculated with Student's *t-test* (**$p < 0.01$).

(C) The relative steady-state level measured by RT–qPCR at 22°C and following low-temperature exposure (12 h at 4°C) of *asAAP1* in WT and *aap1-cr* seedlings grown for 10 days. Steady-state levels were normalized to WT levels at 22°C. The mean values are from three biological replicates. Error bars represent ±SEM. Statistical significance was calculated with Student's *t-test* (*$p < 0.05$).

(D) The relative weight (wet) of WT and *aap1-cr* plants after 5 weeks at 22°C and after 3 weeks at 22°C and 2 weeks at 10°C. Statistical significance was calculated with Student's *t-test* (***$p < 0.001$).

DISCUSSION

An essential prerequisite for a sessile organism is the ability to rapidly and transiently be able to respond to fluctuations in its surrounding environment. In plants, transcriptional regulation of coding and non-coding DNA sequences are a central part of the response. While coding transcription is well studied, non-coding transcription in response to stress is less so. A common form of non-coding transcription in plants occurs on the antisense strand of coding genes (Kindgren et al., 2019; Reis and Poirier, 2021). Antisense transcription has emerged to be an important regulatory element in many developmental and stress-related decisions made by the plant (Reis and Poirier, 2021). Recently, we showed that PASt of specific transcription factors promotes their low-temperature responsiveness (Meena et al., 2024). Here, we characterize another class of antisense transcription in *Arabidopsis*, CASt. In contrast to PASt, CASt initiates in the 5' end of genes. Interestingly, the regulatory functions of CASt in plants seem to differ from metazoans, where they are the dominant form of antisense transcription (Mayer et al., 2015). Plant CASt genes are associated with high transcription activity, while human genes with CAS transcription are mostly lowly expressed (Mayer et al., 2015; Brown et al., 2018). However, no correlation with a long first intron has been investigated in human cells (Mayer et al., 2015; Brown et al., 2018). Exons are phased to nucleosomes, leaving the exon–intron junction at the end of the DNA wrapped around the nucleosome (Andersson et al., 2009; Chodavarapu et al., 2010; Jabre et al., 2021). Consequently, the initial DNA sequence of an intron is less nucleosome rich, and, indeed, the TSS of CASt in *Arabidopsis* is downstream of a nucleosome-depleted region (Kindgren et al., 2019). Although CASt in humans and plants share some features, it is also evident that different organisms have diverging functions for antisense transcription.

We can show that the presence of CASt in *Arabidopsis*, maize, and rice is correlated to the presence of a long first intron and, consequently, host gene stress responsiveness. Our data show a targeted evolution of specific members of AAAP transporters, only one or a few of each subclass have a long first intron and CASt. We experimentally show that part of the first intron of *AAP1* in *Arabidopsis* is responsible for the regulation of CASt (*asAAP1*). The first intron is known to regulate sense expression in plants (Wang et al., 2014; Qüesta et al., 2016), but it is far less known how these sequences determine antisense expression. Previous work has shown that antisense transcription can be either a positive or a negative regulator of sense transcription (Zhao et al., 2018; Zacharaki et al., 2023; Meena et al., 2024). Our work on the *AAP1* locus suggests that *asAAP1* is more important to prime the host gene for low-temperature response rather than regulating sense expression in normal growing conditions, similar to what was found for PASt genes (Meena et al., 2024). It is unlikely that CASt, which is complementary to the mRNA of its host gene, has a direct role in regulating mRNA levels. The CASt is rapidly degraded by the nuclear exosome (Kindgren et al., 2019; Thieffry et al., 2020) and would have limited temporal ability to form double-stranded RNA. In corroboration, our results show that a lower level of *asAAP1* does not affect the stability of *AAP1*. Therefore, a more likely mechanism is that the act of antisense transcription regulates the host genes. For example, antisense transcription has been shown to promote post-translational modifications of histone tails (Qüesta et al., 2016) and the formation of DNA:RNA hybrids (Ariel et al., 2020). Exactly how CASt performs their functions is still unanswered and an obvious avenue for future studies.

In conclusion, the integration of gene architecture with antisense transcription constitutes a conserved mechanism among plant species to diversify functions among gene families to cope with

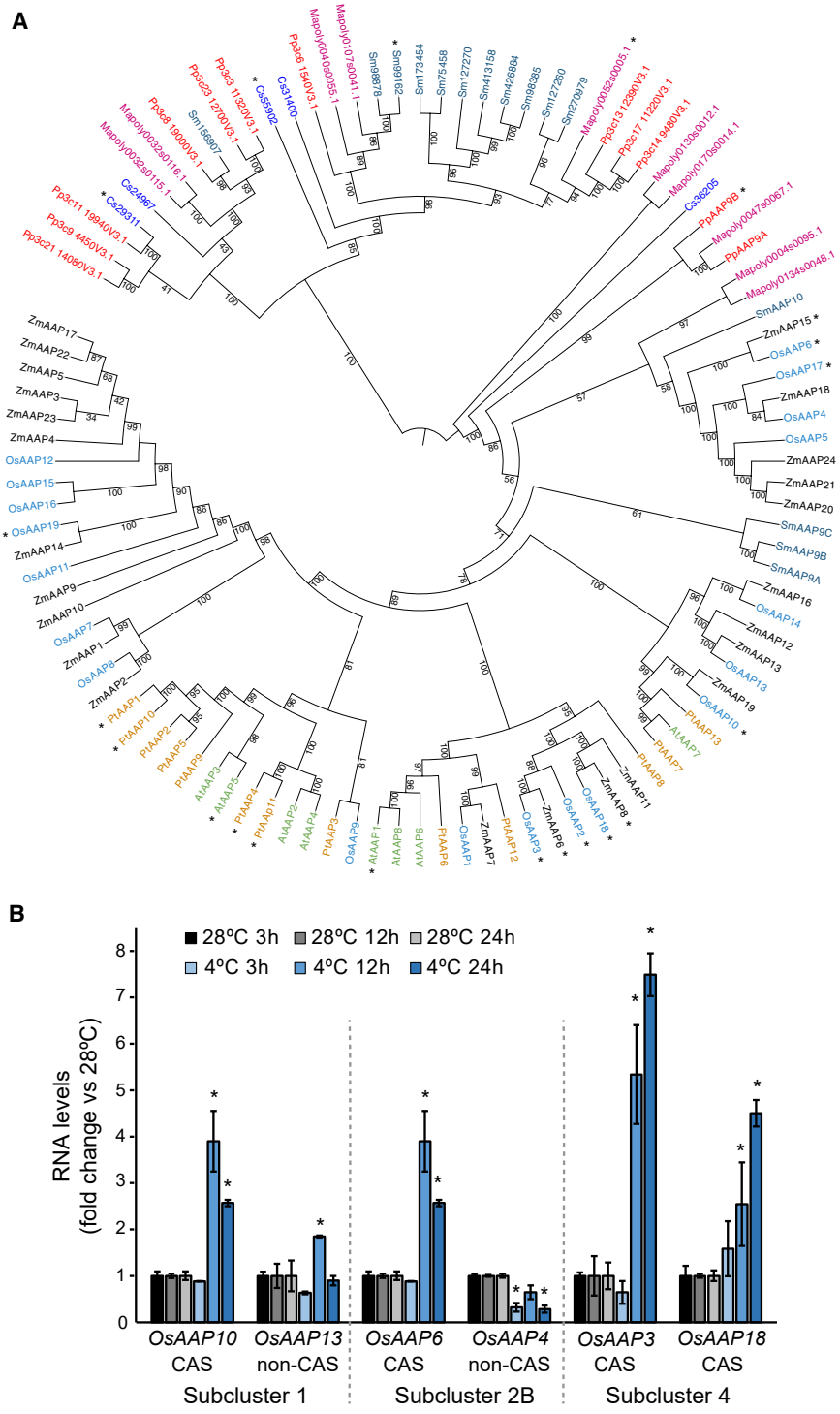

Figure 6. The occurrence of CAS transcription correlates with stress responsiveness in rice.

(A) A phylogenetic tree was reconstructed for AAP proteins of eight plant species from algae to land plants: *Coccomyxa subellipsoidea* (Chlorophyta), *Marchantia polymorpha* (Bryophyta), *Physcomitrella patens* (Bryophyta), *Selaginella moellendorffii* (lycophyte), *Populus trichocarpa* (angiosperms, eudicots), *Arabidopsis thaliana* (angiosperms, eudicots), *Oryza sativa* (angiosperms, monocots), and *Zea mays* (angiosperms, monocots). Each species' loci are denoted by their initial letters and a unique color. Each branch includes a bootstrap value, and proteins encoded by genes with larger first intron are marked with an asterisk (*).

(B) The relative steady-state level measured by RT–qPCR at 28°C and following low-temperature exposure (3, 12, and 24 h at 4°C) of AAP transporters in WT rice seedlings grown for 10 days. Steady-state levels were normalized to each 28°C control time point. The mean values are from three biological replicates. Error bars represent ±SEM. Statistical significance was calculated with Student's *t*-test (*$p < 0.05$).

fluctuating environmental conditions. Antisense transcription coupled with an extended first intron establishes a novel mechanism to prime low-temperature responsiveness in plants.

METHODS

Plant material and growing conditions

Arabidopsis thaliana WT (Col-0) was used in this study. Additional mutants used have been described elsewhere: *aap1-3* (GABI-135G05) (Svennerstam et al., 2011) and *aap5-1* (SALK_041999) (Svennerstam et al., 2008). Seeds were sterilized using 70% ethanol and 0.05% Triton-X, air dried, and sown on ½ MS medium, pH 5.7, 1% sucrose, and 1% agar. Plates were kept in the dark at 4°C for 48 h for stratification and then moved to a growth chamber with 100 $\mu Em^{-2}s^{-1}$ light on long-day (16-h light/8-h dark, 22°C day/18°C night) conditions. 10-day-old seedlings were collected either directly or post low-temperature treatment (4°C with 20–25 $\mu Em^{-2}s^{-1}$ light). Three independent biological replicates were collected, flash-frozen in liquid nitrogen, and stored at −80°C until further use. For weighing of plants at control and 10°C, plants were grown in short-day conditions with 100 $\mu Em^{-2}s^{-1}$ light (8-h light/16-h dark, 22°C day/18°C night) for 3 weeks and then kept at control or transferred to 10°C with similar light conditions. Plants were weighed 14 days after transfer. The *aap1-cr* mutant was created by CRISPR-Cas9 using the pHSE401 binary vector (Xing et al., 2014) and gRNA1 and gRNA2 (Supplemental Table 8). Primers for genotyping the deletion can be found in Supplemental Table 8. Rice seeds from the japonica cultivar (*Oryza sativa* ssp. japonica cv. Nipponbare) were sown in jars on ½ MS medium with vitamins and without sucrose. Seedlings were grown for 10 days (three-leaf stage) in 100 $\mu mol\ m^{-2}\ s^{-1}$ continuous light at 28°C. Half of the jars were then moved to 4°C and sampled in biological triplicates at 3, 12, and 24 h (with the respective controls at 28°C). Only the third active leaf was sampled from seedlings of a similar developmental stage.

RNA extraction, cDNA synthesis, RT–PCR, and qPCR

RNA was extracted with the EZNA Plant RNA Kit (Omega Bio-tek) according to the manufacturer's instructions. Total RNA was DNase treated with

Turbo DNase (Ambion). cDNA synthesis was performed with gene-specific primers with a tag to avoid any residual gDNA amplification and Superscript IV (Invitrogen) to ensure strand specificity (see Supplementary Data 1 for primers). RT–PCR was performed with Phusion polymerase (Thermo Fischer), run on 2% agarose gels, and imaged with a Gel-doc system (Bio-Rad). qPCR reactions were performed with iTaq Universal SYBR Green Supermix (Bio-Rad) in 384-well plates. qPCR was run in a CFX384 Touch Real-Time PCR Detection System (Bio-Rad) and monitored by the CFX Manager software (Bio-Rad). Threshold values were subsequently exported to Excel (Microsoft Office) and further analyzed. For each sample, three independent biological replicates with two to three technical replicates were used. Two internal reference genes (*ACT2* [*AT3G18780*] and *UBQ10* [*AT4G05320*]) were used for relative gene-expression calculations. For rice experiments, 1 μg of total RNA was extracted using the Maxwell RSC Plant RNA Kit (Promega), and first-strand cDNA synthesis was performed using the NZY FirstStrand cDNA Synthesis Kit (NZYTech). Real-time PCR (Light Cycler 480; Roche) using SYBR Premix Ex Taq (Roche) was performed in three independent biological replicates, and at least two technical replicates were used for each of the biological replicates. *OsUBQ* was used as reference. Two-tailed *t*-test was used for all statistical analyses. All primers used in this study can be found in Supplemental Table 8.

Electrolyte-leakage assay

Electrolyte-leakage measurements were done according to a previous study (Kindgren et al., 2015). Briefly, plants were grown in short days (8-h light/16-h dark cycle) for 4 weeks. For the cold-acclimation experiments, WT and mutant plants were transferred to a cold chamber set at 4°C for 4 days without changing photoperiodic conditions. Randomized leaf disks of 1-cm diameter, for each genotype in triplicates from several similar sized leaves, were prepared for acclimated or non-acclimated plants and carefully placed horizontally in clean glass tubes filled with 200 μl of deionized distilled water so that the leaf disks touched the water. Tubes containing two leaf disks were then transferred to a programmable freezing bath (FP51, Julabo, Germany) set at −2° C. After 60 min, icing was induced manually in each tube with the help of liquid N_2 and a metallic stick. Temperature decrease occurred at the rate of −1°C per 30 min, and samples were taken out at designated temperature point(s) followed by incubation on ice for at least 1 h in the cold room (4°C). Subsequently, 1.3 mL of water was added to each tube and placed on a shaker overnight, and conductivity was measured using a conductivity cell (CDM210, Radiometer, Denmark) on the next day. Finally, all tubes were subjected to flash freeze using liquid N_2 and left on a shaker overnight at room temperature. To obtain the total electrolyte content from leaf disks, conductivity was measured again, and the percentage of electrolyte leakage was calculated using the following formula: (conductivity before flash freeze/conductivity after flash freeze) × 100. Data were fitted into a sigmoidal dose-response curve using GraphPad Prism software, and significant differences in the fit were determined with an extra sum-of-squares F test.

RNA-stability assay

RNA-stability measurements to determine the half-life (t1/2) of transcripts were performed according to the previous report (Fedak et al., 2016). In summary, 10-day-old WT seedlings were grown in a long-day photoperiod (16-h light/8-h dark, 22°C day/18°C night) over ½ MS medium supplemented with 1% sucrose (w/v). On day 10, seedlings were transferred to liquid ½ MS medium and acclimatized while maintaining 22°C or 4°C growth temperatures for respective sample sets under the same light conditions. Further, samples from 22°C or 4°C were transferred to incubation buffer (1 mM PIPES at pH 6.25, 1 mM trisodium citrate, 1 mM KCl, and 15 mM sucrose) in 12-well plates for 30 min followed by the addition of 150 mg/l cordycepin (3′-deoxyadenosine, Sigma Aldrich). Immediately after cordycepin addition, samples were vacuum infiltrated (5 min two times). 15 seedlings for each of the samples in triplicates were collected at 0, 15, 30, 60, and 120 min after cordycepin treatment. Subsequently, total RNA extraction and strand-specific RT–qPCR analyses were carried out by using cDNA as a template synthesized with SuperScript IV Reverse Transcriptase (Invitrogen) and gene-specific primers. *EUKARYOTIC TRANSLATION INITIATION FACTOR 4A1* (*EIF4A1* and *AT3G13920*) was used as an internal assay control. Cq values at 15, 30, 60, and 120 min were normalized with Cq at 0 min and the RNA degradation curve obtained following the equation [Cq(n) = (ln (Cq/Cq (0)) × (−10)]. Finally, t1/2 of transcripts were calculated from the obtained slope [t1/2 = (ln2)/slope]. The oligos used can be found in Supplemental Table 8.

RGR experiment

RGR experiments were performed according to Nunes et al. (2013). Briefly, seedlings grew with 0.5% (w/v) sucrose for 7 days at 22°C (t-24h), after which medium was changed and either transferred to 4°C for 24 h and then back to 22°C or held at 22°C throughout. Harvests were all performed at 22°C and at time points −24, 0, 4, 11, 24, and 48 h starting at ZT4 (t0). Five plants were harvested for each replicate and time point. Medium change was performed 4 h after the start of the light period. The RGR was calculated using the method indicated by Hoffmann and Poorter (2002).

Targeted metabolites measurement

Col-0, *aap1-3*, and *aap5-1* seeds were surface sterilized and grown under long-day conditions for 10 days. On day 10, half of the seedlings were exposed to low temperature (4°C with 20–25 $\mu Em^{-2s^{-1}}$ light) for 3 h while the rest remained at 22°C. Seedlings were sampled at the end of the 3 h for both conditions. The samples were ground to a fine powder and weighed. 20 mg of fine-ground tissue was used for polyamine quantification, with five biological replications per condition and genotype and two technical replicates for each sample. Samples were extracted, analyzed, and run in a randomized order as previously described (Liebsch et al., 2022). Quality controls for the metabolite analysis were similar to Liebsch et al. (2022). Metabolite extraction and analysis was performed by the Swedish Metabolomics Center, Umeå, Sweden.

Genome-wide analyses

Detailed bioinformatic methods can be accessed at https://github.com/peterkindgrengroup/Zacharaki-et-al-2024. Briefly, a control set of genes without CAS transcription was curated from all expressed genes (22°C RNA-seq data; Meena et al., 2024). For RNA-expression analysis, we normalized values using the *Z* score method and compared the expression of the different subsets of genes. To better define the gene coordinates of both controls and CASt genes, we used TSS sequencing data from Table S4 in Nielsen et al. (2019) in combination with the TTS from TAIR10. Gene length was calculated from these curated genomic features. For intron analysis, we used Araport11 annotation (Cheng et al., 2017) to curate the first-intron whole-genome dataset (available at GitHub). Next, we subset control genes and CASt genes to calculate the mean length of the first introns. A set of control genes with similar expression levels and first-intron length as the whole CASt subset was curated to correct for these variables when studying chromatin features. Publicly available data (bigwig files) for ATAC-seq (GSM6062224) (Liang et al., 2024) were retrieved from Gene Expression Omnibus. Bedgraphs from samples GSM2522253 for PolII_WT were converted to bigwig (Kent et al., 2010). Deeptools (Ramírez et al., 2016) was used to compute chromatin immunoprecipitation sequencing score matrices and to generate metaplots along the gene body. PhyloP conservation scores for *Arabidopsis* calculated from 65 plants were downloaded from the PlantRegMap database (Tian et al., 2019) and used to plot the average sequence conservation of the region surrounding each TSS using deeptools (the 63 plant species used in the analysis can be found in Supplemental Table 9). To build the plaNET-seq metaplots, the raw sequences (SRR9117170-SRR9117181) were downloaded from GSE131733 (Kindgren et al., 2019) and processed as indicated in the GitHub repository. The differentially expressed genes from this published plaNET-seq study were also used in our analysis. As described in GitHub,

the bam files were generated using STAR 2.7.10a (Dobin et al., 2012), and ngs.plot (Shen et al., 2014) was used to generate the metagene profiles using the in-built TAIR10 genome and the gene lists of interest. CAGE (Thieffry et al., 2020) and DRS sequencing data (Schurch et al., 2014) were obtained from earlier studies.

Phylogenetic analysis of AAP

The protein and genomic sequences for the AAPs of the seven selected species, *Coccomyxa subellipsoidea*, *Physcomitrella patens*, *Marchantia polymorpha*, *Selaginella moellendorffii*, *Arabidopsis thaliana*, *Oryza sativa*, *Populus trichocarpa*, and *Zea mays* were obtained from the Phytozome website (version 13) (Goodstein et al., 2011). Phylogenetic inference was performed using protein sequences. Initially, the protein sequences underwent alignment using MAFFT software (version 7) (Rozewicki et al., 2019), and phylogenies were reconstructed in Iqtree software (version 2.3.4) (Nguyen et al., 2014) utilizing likelihood methodology with 1000 bootstrap replications to establish branch-support values. The reconstructed tree was then visualized using the Interactive Tree of Life software (Itol, version 6) (Letunic and Bork, 2024). Finally, the sizes of the first introns were assessed in the retrieved genomic sequences and annotated with asterisks (*) in the reconstructed tree.

FUNDING

The research in the P.K. lab was funded by the Swedish Research Council (2018-03926), Formas (2021-01065), Carl Trygger Foundation (20:224), and grants from the Knut and Alice Wallenberg Foundation and the Swedish Governmental Agency for Innovation Systems (KAW 2016.0355 and 2020.0240, VINNOVA 2016-00504). Grants and financial support was provided to E.M. from FEDER/Ministerio de Ciencia, Innovación y Universidades – Agencia Estatal de Investigación (PID2021-122288NB-I00); from the CERCA Programme/Generalitat de Catalunya (2021SGR-792), and from the Spanish Ministry of Economy and Competitiveness through the Severo Ochoa Programme for Centers of Excellence in CEX2019-000902-S funded by MCIN/AEI/10.13039/501100011033. M.Q. received postdoctoral funding from the European Union's Horizon 2020 research and innovation program under the Marie Skłodowska-Curie grant agreement no. 945043.

ACKNOWLEDGMENTS

We would like to thank members of the Kindgren lab for their critical reading of the manuscript. We would like to thank the greenhouse personnel at Umeå Plant Science Center for plant maintenance and Nicolas Delhomme for bioinformatic help. No conflict of interest is declared .

AUTHOR CONTRIBUTIONS

V.Z., M.Q., S.M.N., S.K.M., and P.K. designed the research. V.Z., M.Q., S.M.N., S.K.M., and P.K. performed research. V.Z., M.Q., S.M.N., S.K.M., and P.K. analyzed data. V.Z., M.Q., S.M.N., S.K.M., E.M., and P.K. wrote the paper. E.M. and P.K. supervised research.

SUPPLEMENTAL INFORMATION

Supplemental information is available at *Molecular Plant Online*.

Received: May 5, 2025
Revised: September 8, 2025
Accepted: October 1, 2025
Published: October 4, 2025

REFERENCES

Ahn, S.J., Shin, R., and Schachtman, D.P. (2004). Expression of KT/KUP genes in Arabidopsis and the role of root hairs in K+ uptake. Plant Physiol. **134**:1135–1145. https://doi.org/10.1104/pp.103.034660.

Andersson, R., Enroth, S., Rada-Iglesias, A., Wadelius, C., and Komorowski, J. (2009). Nucleosomes are well positioned in exons and carry characteristic histone modifications. Genome Res. **19**:1732–1741. https://doi.org/10.1101/gr.092353.109.

Ariel, F., Lucero, L., Christ, A., Mammarella, M.F., Jegu, T., Veluchamy, A., Mariappan, K., Latrasse, D., Blein, T., Liu, C., et al. (2020). R-Loop Mediated trans Action of the APOLO Long Noncoding RNA. Mol. Cell **77**:1055–1065.e4. https://doi.org/10.1016/j.molcel.2019.12.015.

Bai, X., Xu, J., Shao, X., Luo, W., Niu, Z., Gao, C., and Wan, D. (2019). A Novel Gene Coding γ-Aminobutyric Acid Transporter May Improve the Tolerance of Populus euphratica to Adverse Environments. Front. Plant Sci. **10**:1083. https://doi.org/10.3389/fpls.2019.01083.

Barand, A., Nasibi, F., and ManouchehriKalantari, K. (2015). The effect of arginine pretreatment in the increase of cold tolerance in Pistacia vera L. in vitro. Russ. Agric. Sci. **41**:340–346. https://doi.org/10.3103/S1068367415050043.

Blázquez, M.A. (2024). Polyamines: Their Role in Plant Development and Stress. Annu. Rev. Plant Biol. **75**:95–117. https://doi.org/10.1146/annurev-arplant-070623-110056.

Boorer, K.J., and Fischer, W.-N. (1997). Specificity and Stoichiometry of the ArabidopsisH+/Amino Acid Transporter AAP5. J. Biol. Chem. **272**:13040–13046. https://doi.org/10.1074/jbc.272.20.13040.

Brown, T., Howe, F.S., Murray, S.C., Wouters, M., Lorenz, P., Seward, E., Rata, S., Angel, A., and Mellor, J. (2018). Antisense transcription-dependent chromatin signature modulates sense transcript dynamics. Mol. Syst. Biol. **14**:e8007. https://doi.org/10.15252/msb.20178007.

Chen, D., Shao, Q., Yin, L., Younis, A., and Zheng, B. (2019). Polyamine Function in Plants: Metabolism, Regulation on Development, and Roles in Abiotic Stress Responses. Front. Plant Sci. **9**:1945. https://doi.org/10.3389/fpls.2018.01945.

Cheng, C.-Y., Krishnakumar, V., Chan, A.P., Thibaud-Nissen, F., Schobel, S., and Town, C.D. (2017). Araport11: a complete reannotation of the Arabidopsis thaliana reference genome. Plant J. **89**:789–804. https://doi.org/10.1111/tpj.13415.

Chodavarapu, R.K., Feng, S., Bernatavichute, Y.V., Chen, P.Y., Stroud, H., Yu, Y., Hetzel, J.A., Kuo, F., Kim, J., Cokus, S.J., et al. (2010). Relationship between nucleosome positioning and DNA methylation. Nature **466**:388–392. https://doi.org/10.1038/nature09147.

Churchman, L.S., and Weissman, J.S. (2011). Nascent transcript sequencing visualizes transcription at nucleotide resolution. Nature **469**:368–373. https://doi.org/10.1038/nature09652.

Denancé, N., Szurek, B., and Noël, L.D. (2014). Emerging Functions of Nodulin-Like Proteins in Non-Nodulating Plant Species. Plant Cell Physiol. **55**:469–474. https://doi.org/10.1093/pcp/pct198.

Dobin, A., Davis, C.A., Schlesinger, F., Drenkow, J., Zaleski, C., Jha, S., Batut, P., Chaisson, M., and Gingeras, T.R. (2013). STAR: ultrafast universal RNA-seq aligner. Bioinformatics **29**:15–21. https://doi.org/10.1093/bioinformatics/bts635.

Fedak, H., Palusinska, M., Krzyczmonik, K., Brzezniak, L., Yatusevich, R., Pietras, Z., Kaczanowski, S., and Swiezewski, S. (2016). Control of seed dormancy in Arabidopsis by a cis-acting noncoding antisense transcript. Proc. Natl. Acad. Sci. USA **113**:E7846–E7855. https://doi.org/10.1073/pnas.1608827113.

Fischer, W., André, B., Rentsch, D., Krolkiewicz, S., Tegeder, M., Breitkreuz, K., and Frommer, W.B. (1998). Amino acid transport in plants. Trends Plant Sci. **3**:188–195. https://doi.org/10.1016/S1360-1385(98)01231-X.

Gilmour, S.J., Sebolt, A.M., Salazar, M.P., Everard, J.D., and Thomashow, M.F. (2000). Overexpression of the Arabidopsis CBF3 transcriptional activator mimics multiple biochemical changes associated with cold acclimation. Plant Physiol. **124**:1854–1865. https://doi.org/10.1104/pp.124.4.1854.

Gong, Z., Koiwa, H., Cushman, M.A., Ray, A., Bufford, D., Kore-eda, S., Matsumoto, T.K., Zhu, J., Cushman, J.C., Bressan, R.A., and Hasegawa, P.M. (2001). Genes That Are Uniquely Stress Regulated

in Salt Overly Sensitive (sos) Mutants. Plant Physiol. **126**:363–375. https://doi.org/10.1104/pp.126.1.363.

Goodstein, D.M., Shu, S., Howson, R., Neupane, R., Hayes, R.D., Fazo, J., Mitros, T., Dirks, W., Hellsten, U., Putnam, N., et al. (2012). Phytozome: a comparative platform for green plant genomics. Nucleic Acids Res. **40**:D1178–D1186. https://doi.org/10.1093/nar/gkr944.

Hao, D.L., Zhou, J.Y., Yang, S.Y., Qi, W., Yang, K.J., and Su, Y.H. (2020). Function and Regulation of Ammonium Transporters in Plants. Int. J. Mol. Sci. **21**:3557. https://doi.org/10.3390/ijms21103557.

Hoffmann, W.A., and Poorter, H. (2002). Avoiding Bias in Calculations of Relative Growth Rate. Ann. Bot. **90**:37–42. https://doi.org/10.1093/aob/mcf140.

Islam, M.N., Rabby, M.G., Hossen, M.M., Bonny, M., and Hasan, M.M. (2024). Genome-wide identification following functional analysis of amino acid permease and cationic amino acid transporter gene families in maize and their role in drought stress. South Afr. J. Bot. **168**:360–371. https://doi.org/10.1016/j.sajb.2024.03.029.

Jabre, I., Reddy, A.S.N., Kalyna, M., Chaudhary, S., Khokhar, W., Byrne, L.J., Wilson, C.M., and Syed, N.H. (2019). Does co-transcriptional regulation of alternative splicing mediate plant stress responses? Nucleic Acids Res. **47**:2716–2726. https://doi.org/10.1093/nar/gkz121.

Jabre, I., Chaudhary, S., Guo, W., Kalyna, M., Reddy, A.S.N., Chen, W., Zhang, R., Wilson, C., and Syed, N.H. (2021). Differential nucleosome occupancy modulates alternative splicing in Arabidopsis thaliana. New Phytol. **229**:1937–1945. https://doi.org/10.1111/nph.17062.

Jaglo-Ottosen, K.R., Gilmour, S.J., Zarka, D.G., Schabenberger, O., and Thomashow, M.F. (1998). Arabidopsis CBF1 Overexpression Induces COR Genes and Enhances Freezing Tolerance. Science **280**:104–106. https://doi.org/10.1126/science.280.5360.104.

Jelesko, J.G. (2012). An expanding role for purine uptake permease-like transporters in plant secondary metabolism. Front. Plant Sci. **3**:78. https://doi.org/10.3389/fpls.2012.00078.

Ji, J., Yang, L., Fang, Z., Zhang, Y., Zhuang, M., Lv, H., and Wang, Y. (2022). Plant SWEET Family of Sugar Transporters: Structure, Evolution and Biological Functions. Biomolecules **12**:205.

Jo, S.-S., and Choi, S.S. (2019). Analysis of the Functional Relevance of Epigenetic Chromatin Marks in the First Intron Associated with Specific Gene Expression Patterns. Genome Biol. Evol. **11**:786–797. https://doi.org/10.1093/gbe/evz033.

Joly-Lopez, Z., Platts, A.E., Gulko, B., Choi, J.Y., Groen, S.C., Zhong, X., Siepel, A., and Purugganan, M.D. (2020). An inferred fitness consequence map of the rice genome. Nat. Plants **6**:119–130. https://doi.org/10.1038/s41477-019-0589-3.

Kang, J., Park, J., Choi, H., Burla, B., Kretzschmar, T., Lee, Y., and Martinoia, E. (2011). Plant ABC Transporters. Arabidopsis Book **9**: e0153. https://doi.org/10.1199/tab.0153.

Kent, W.J., Zweig, A.S., Barber, G., Hinrichs, A.S., and Karolchik, D. (2010). BigWig and BigBed: enabling browsing of large distributed datasets. Bioinformatics **26**:2204–2207. https://doi.org/10.1093/bioinformatics/btq351.

Kindgren, P., Dubreuil, C., and Strand, Å. (2015). The Recovery of Plastid Function Is Required for Optimal Response to Low Temperatures in Arabidopsis. PLoS One **10**:e0138010. https://doi.org/10.1371/journal.pone.0138010.

Kindgren, P., Ivanov, M., and Marquardt, S. (2020). Native elongation transcript sequencing reveals temperature dependent dynamics of nascent RNAPII transcription in Arabidopsis. Nucleic Acids Res. **48**:2332–2347. https://doi.org/10.1093/nar/gkz1189.

Le Hir, H., Nott, A., and Moore, M.J. (2003). How introns influence and enhance eukaryotic gene expression. Trends Biochem. Sci. **28**:215–220. https://doi.org/10.1016/S0968-0004(03)00052-5.

Lee, H.J., Lee, J.H., Wi, S., Jang, Y., An, S., Choi, C.K., and Jang, S. (2021). Exogenously applied glutamic acid confers improved yield through increased photosynthesis efficiency and antioxidant defense system under chilling stress condition in Solanum lycopersicum L. cv. Dotaerang Dia. Sci. Hortic. **277**:109817. https://doi.org/10.1016/j.scienta.2020.109817.

Lee, Y.H., Foster, J., Chen, J., Voll, L.M., Weber, A.P.M., and Tegeder, M. (2007). AAP1 transports uncharged amino acids into roots of Arabidopsis. Plant J. **50**:305–319. https://doi.org/10.1111/j.1365-313X.2007.03045.x.

Letunic, I., and Bork, P. (2024). Interactive Tree of Life (iTOL) v6: recent updates to the phylogenetic tree display and annotation tool. Nucleic Acids Res. **52**:W78–W82. https://doi.org/10.1093/nar/gkae268.

Li, L., He, Z., Pandey, G.K., Tsuchiya, T., and Luan, S. (2002). Functional Cloning and Characterization of a Plant Efflux Carrier for Multidrug and Heavy Metal Detoxification. J. Biol. Chem. **277**:5360–5368. https://doi.org/10.1074/jbc.M108777200.

Liang, Z., Zhu, T., Yu, Y., Wu, C., Huang, Y., Hao, Y., Song, X., Fu, W., Yuan, L., Cui, Y., et al. (2024). PICKLE-mediated nucleosome condensing drives H3K27me3 spreading for the inheritance of Polycomb memory during differentiation. Mol. Cell **84**:3438–3454.e8. https://doi.org/10.1016/j.molcel.2024.08.018.

Liebsch, D., Juvany, M., Li, Z., Wang, H.L., Ziolkowska, A., Chrobok, D., Boussardon, C., Wen, X., Law, S.R., Janečková, H., et al. (2022). Metabolic control of arginine and ornithine levels paces the progression of leaf senescence. Plant Physiol. **189**:1943–1960. https://doi.org/10.1093/plphys/kiac244.

Lozano, R., Booth, G.T., Omar, B.Y., Li, B., Buckler, E.S., Lis, J.T., del Carpio, D.P., and Jannink, J.-L. (2021). RNA polymerase mapping in plants identifies intergenic regulatory elements enriched in causal variants. G3 Genes **11**:jkab273. https://doi.org/10.1093/g3journal/jkab273.

Mastrangelo, A.M., Marone, D., Laidò, G., De Leonardis, A.M., and De Vita, P. (2012). Alternative splicing: Enhancing ability to cope with stress via transcriptome plasticity. Plant Sci. **185–186**:40–49. https://doi.org/10.1016/j.plantsci.2011.09.006.

Maurino, V.G., Grube, E., Zielinski, J., Schild, A., Fischer, K., and Flügge, U.-I. (2006). Identification and Expression Analysis of Twelve Members of the Nucleobase–Ascorbate Transporter (NAT) Gene Family in Arabidopsis thaliana. Plant Cell Physiol. **47**:1381–1393. https://doi.org/10.1093/pcp/pcl011.

Mayer, A., di Iulio, J., Maleri, S., Eser, U., Vierstra, J., Reynolds, A., Sandstrom, R., Stamatoyannopoulos, J.A., and Churchman, L.S. (2015). Native elongating transcript sequencing reveals human transcriptional activity at nucleotide resolution. Cell **161**:541–554. https://doi.org/10.1016/j.cell.2015.03.010.

Meena, S.K., Quevedo, M., Nardeli, S.M., Verez, C., Bhat, S.S., Zacharaki, V., and Kindgren, P. (2024). Antisense transcription from stress-responsive transcription factors fine-tunes the cold response in Arabidopsis. Plant Cell **36**:3467–3482. https://doi.org/10.1093/plcell/koae160.

Nguyen, L.-T., Schmidt, H.A., von Haeseler, A., and Minh, B.Q. (2015). IQ-TREE: A Fast and Effective Stochastic Algorithm for Estimating Maximum-Likelihood Phylogenies. Mol. Biol. Evol. **32**:268–274. https://doi.org/10.1093/molbev/msu300.

Nielsen, M., Ard, R., Leng, X., Ivanov, M., Kindgren, P., Pelechano, V., and Marquardt, S. (2019). Transcription-driven chromatin repression of Intragenic transcription start sites. PLoS Genet. **15**:e1007969. https://doi.org/10.1371/journal.pgen.1007969.

Niño-González, M., Novo-Uzal, E., Richardson, D.N., Barros, P.M., and Duque, P. (2019). More Transporters, More Substrates: The Arabidopsis Major Facilitator Superfamily Revisited. Mol. Plant **12**:1182–1202. https://doi.org/10.1016/j.molp.2019.07.003.

Nunes, C., O'Hara, L.E., Primavesi, L.F., Delatte, T.L., Schluepmann, H., Somsen, G.W., Silva, A.B., Fevereiro, P.S., Wingler, A., and Paul, M.J. (2013). The Trehalose 6-Phosphate/SnRK1 Signaling Pathway Primes Growth Recovery following Relief of Sink Limitation. Plant Physiol. **162**:1720–1732. https://doi.org/10.1104/pp.113.220657.

Park, S.G., Hannenhalli, S., and Choi, S.S. (2014). Conservation in first introns is positively associated with the number of exons within genes and the presence of regulatory epigenetic signals. BMC Genom. **15**:526. https://doi.org/10.1186/1471-2164-15-526.

Perchlik, M., Foster, J., and Tegeder, M. (2014). Different and overlapping functions of Arabidopsis LHT6 and AAP1 transporters in root amino acid uptake. J. Exp. Bot. **65**:5193–5204. https://doi.org/10.1093/jxb/eru278.

Qüesta, J.I., Song, J., Geraldo, N., An, H., and Dean, C. (2016). Arabidopsis transcriptional repressor VAL1 triggers Polycomb silencing at FLC during vernalization. Science **353**:485–488. https://doi.org/10.1126/science.aaf7354.

Ramazan, S., Nazir, I., Yousuf, W., and John, R. (2023). Environmental stress tolerance in maize (Zea mays): role of polyamine metabolism. Funct. Plant Biol. **50**:85–96. https://doi.org/10.1071/fp21324.

Ramírez, F., Ryan, D.P., Grüning, B., Bhardwaj, V., Kilpert, F., Richter, A.S., Heyne, S., Dündar, F., and Manke, T. (2016). deepTools2: a next generation web server for deep-sequencing data analysis. Nucleic Acids Res. **44**:W160–W165. https://doi.org/10.1093/nar/gkw257.

Reis, R.S., and Poirier, Y. (2021). Making sense of the natural antisense transcript puzzle. Trends Plant Sci. **26**:1104–1115. https://doi.org/10.1016/j.tplants.2021.07.004.

Rozewicki, J., Li, S., Amada, K.M., Standley, D.M., and Katoh, K. (2019). MAFFT-DASH: integrated protein sequence and structural alignment. Nucleic Acids Res. **47**:W5–W10. https://doi.org/10.1093/nar/gkz342.

Schurch, N.J., Cole, C., Sherstnev, A., Song, J., Duc, C., Storey, K.G., McLean, W.H.I., Brown, S.J., Simpson, G.G., and Barton, G.J. (2014). Improved Annotation of 3′ Untranslated Regions and Complex Loci by Combination of Strand-Specific Direct RNA Sequencing, RNA-Seq and ESTs. PLoS One **9**:e94270. https://doi.org/10.1371/journal.pone.0094270.

Shen, L., Shao, N., Liu, X., and Nestler, E. (2014). ngs.plot: Quick mining and visualization of next-generation sequencing data by integrating genomic databases. BMC Genom. **15**:284. https://doi.org/10.1186/1471-2164-15-284.

Svennerstam, H., Ganeteg, U., and Näsholm, T. (2008). Root uptake of cationic amino acids by Arabidopsis depends on functional expression of amino acid permease 5. New Phytol. **180**:620–630. https://doi.org/10.1111/j.1469-8137.2008.02589.x.

Svennerstam, H., Jämtgård, S., Ahmad, I., Huss-Danell, K., Näsholm, T., and Ganeteg, U. (2011). Transporters in Arabidopsis roots mediating uptake of amino acids at naturally occurring concentrations. New Phytol. **191**:459–467. https://doi.org/10.1111/j.1469-8137.2011.03699.x.

Taylor, M.R., Reinders, A., and Ward, J.M. (2015). Transport Function of Rice Amino Acid Permeases (AAPs). Plant Cell Physiol. **56**:1355–1363. https://doi.org/10.1093/pcp/pcv053.

Tegeder, M., and Ward, J.M. (2012). Molecular Evolution of Plant AAP and LHT Amino Acid Transporters. Front. Plant Sci. **3**:21. https://doi.org/10.3389/fpls.2012.00021.

Thieffry, A., Vigh, M.L., Bornholdt, J., Ivanov, M., Brodersen, P., and Sandelin, A. (2020). Characterization of Arabidopsis thaliana Promoter Bidirectionality and Antisense RNAs by Inactivation of Nuclear RNA Decay Pathways. Plant Cell **32**:1845–1867. https://doi.org/10.1105/tpc.19.00815.

Tian, F., Yang, D.-C., Meng, Y.-Q., Jin, J., and Gao, G. (2020). PlantRegMap: charting functional regulatory maps in plants. Nucleic Acids Res. **48**:D1104–D1113. https://doi.org/10.1093/nar/gkz1020.

Wang, Y., Fan, X., Lin, F., He, G., Terzaghi, W., Zhu, D., and Deng, X.W. (2014). Arabidopsis noncoding RNA mediates control of photomorphogenesis by red light. Proc. Natl. Acad. Sci. USA **111**:10359–10364. https://doi.org/10.1073/pnas.1409457111.

Xing, H.-L., Dong, L., Wang, Z.-P., Zhang, H.-Y., Han, C.-Y., Liu, B., Wang, X.-C., and Chen, Q.-J. (2014). A CRISPR/Cas9 toolkit for multiplex genome editing in plants. BMC Plant Biol. **14**:327. https://doi.org/10.1186/s12870-014-0327-y.

Zacharaki, V., Meena, S.K., and Kindgren, P. (2023). The non-coding RNA SVALKA locus produces a cis-natural antisense transcript that negatively regulates the expression of CBF1 and biomass production at normal temperatures. Plant Commun. **4**:100551. https://doi.org/10.1016/j.xplc.2023.100551.

Zalabák, D., and Ikeda, Y. (2020). First Come, First Served: Sui Generis Features of the First Intron. Plants **9**:911.

Zhang, C., Kong, N., Cao, M., Wang, D., Chen, Y., and Chen, Q. (2020). Evolutionary significance of amino acid permease transporters in 17 plants from Chlorophyta to Angiospermae. BMC Genom. **21**:391. https://doi.org/10.1186/s12864-020-6729-3.

Zhao, X., Li, J., Lian, B., Gu, H., Li, Y., and Qi, Y. (2018). Global identification of Arabidopsis lncRNAs reveals the regulation of MAF4 by a natural antisense RNA. Nat. Commun. **9**:5056. https://doi.org/10.1038/s41467-018-07500-7.